Single Unlabeled Protein Detection on Individual Plasmonic Nanoparticles

ARTICLE *in* NANO LETTERS · FEBRUARY 2012

Impact Factor: 13.59 · DOI: 10.1021/nl204496g · Source: PubMed

NANO LETTERS

Letter

pubs.acs.org/NanoLett

Single Unlabeled Protein Detection on Individual Plasmonic Nanoparticles

Irene Ament,[†] Janak Prasad,[†,‡] Andreas Henkel,[†] Sebastian Schmachtel,[†] and Carsten Sönnichsen*[,†]

[†]Institute for Physical Chemistry, University of Mainz, D-55128 Mainz, Germany

[‡]Graduate School Materials Science in Mainz, Staudingerweg 9, D-55128 Mainz, Germany

Supporting Information

ABSTRACT: The ultimate detection limit in analytic chemistry and biology is the single molecule. Commonly, fluorescent dye labels or enzymatic amplification are employed. This requires additional labeling of the analyte, which modifies the species under investigation and therefore influences biological processes. Here, we utilize single gold nanoparticles to detect single unlabeled proteins with extremely high temporal resolution. This allows for monitoring the dynamic evolution of a single protein binding event on a millisecond time scale. The technique even resolves equilibrium coverage fluctuations, opening a window into Brownian dynamics of unlabeled macromolecules. Therefore, our method enables the study of protein folding dynamics, protein adsorption processes, and kinetics as well as nonequilibrium soft matter dynamics on the single molecule level.

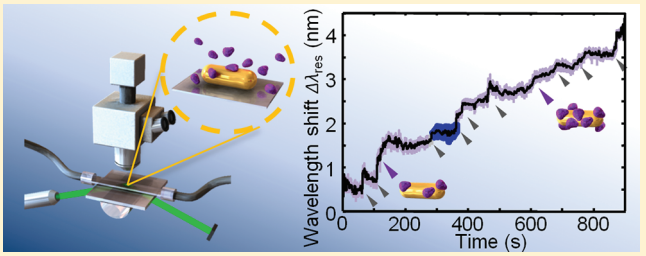

KEYWORDS: *Plasmon sensor, single molecule detection, adsorption dynamics, coverage fluctuations*

Mostly hidden to us, dissolved molecules show complex conformational dynamics, molecular interactions, and spatial diffusion at room temperature. Many of those features average out in measurements integrating over time or large ensembles of molecules. Knowing the detailed dynamics is essential to understand biological functions at the molecular level.[1] However, few experimental techniques provide access to molecular events in solution and commonly require fluorescent dye labels attached to the molecule of interest.[2] Analyte modification could potentially influence biological processes[3] triggering current searches for unlabeled protein detection methods. Currently optical microcavities (whispering gallery modes WGM),[4,5,33] surface-enhanced Raman scattering (SERS),[6] optical trapping in nanoholes,[34] and electric detection via carbon nanotube[7] or boron-doped silicon nanowire[8] field-effect transistors are discussed for detection of unlabeled proteins. Each of these methods suffers from one or more disadvantages, e.g., complex sensor fabrication or low signal-to-noise level, which has prevented their practical use in most cases. Here, we utilize single gold nanoparticles to detect single unlabeled proteins with high temporal resolution. In comparison with previously described techniques, the signal-to-noise ratio is significantly improved and allows the direct identification of single molecular binding and unbinding events. This allows now to resolve equilibrium coverage fluctuations otherwise hidden in ensemble measurements. Plasmonic sensors open new experimental access to the exciting Brownian dynamics of unlabeled macromolecules. Potentially, our method enables the study of protein folding dynamics, protein adsorption processes, and kinetics as well as nonequilibrium soft matter dynamics on the single molecule level. Our simulations predict the ability of the sensor concept to detect the presence of small molecules below a molecular weight of 1 kDa.

Plasmonic nanoparticles[9−11] react to refractive index changes in their direct environment by a shift of the plasmon resonance (Figure 1a). This can be monitored on single nanoparticles by optical dark-field spectroscopy.[12] So far, signal-to-noise ratio and time resolution were not sufficient to identify single molecular binding events. We improved the plasmon spectroscopy technique considerably by using an intense light source (white light laser), an intensified CCD camera, and a tailored nanoparticle geometry. These changes allow for continuous monitoring of very small changes in the plasmon resonance wavelength with a time resolution at least 4−6 orders of magnitude better than the previous state of the art (Figure 1b). These improvements allow us to resolve discrete steps in the plasmon wavelength which are caused by single adsorbing molecules (Figure 1c).

With these advances to plasmon sensors, we introduce a new tool for label-free single molecule detection. Compared to optical microcavities,[13] the plasmon sensor benefits from its less complex optical setup and simple wet-chemical sensor fabrication. In addition, the volume influencing the sensor is orders of magnitude better matched to typical molecular dimensions of proteins. Also, plasmonic nanoparticles can be

Received: December 21, 2011
Revised: January 17, 2012
Published: January 23, 2012

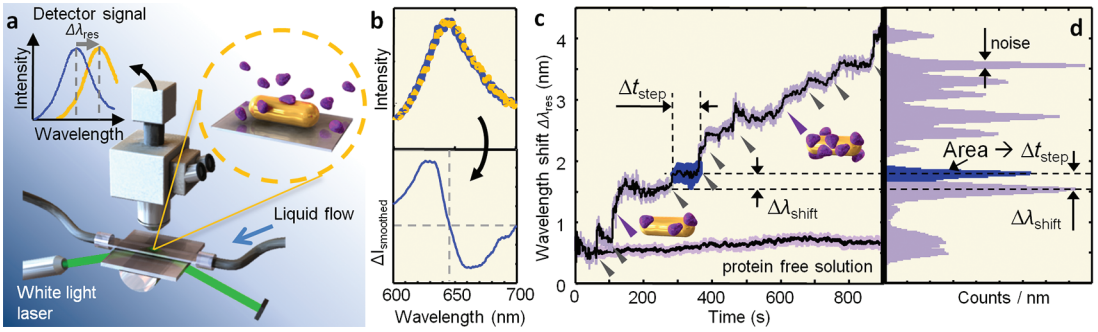

Figure 1. Experimental setup and time-resolved single protein attachment. (a) Diagram of our total internal reflection setup with a magnified view of the flow cell. The inset on the upper left illustrates the plasmonic wavelength shift at the heart of our sensing principle. (b) Measured resonance spectrum of a single Au nanorod with an exposure time of 10 ms before and after single protein attachment (upper panel) and the difference between both (lower panel). (c) Resonance wavelength of an individual nanorod during single protein attachment events and in protein free solution. (d) Histogram of the same time trace showing distinct peaks for each step.

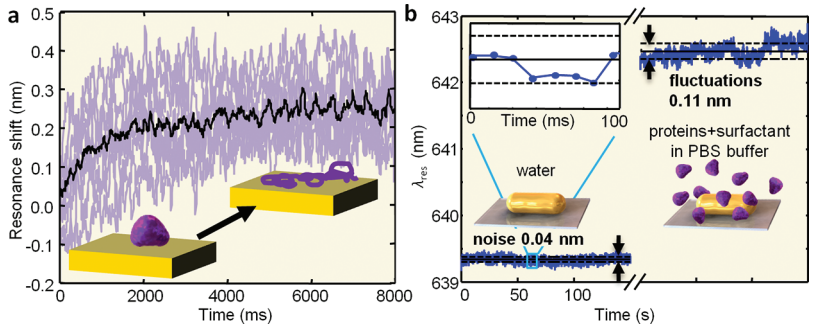

Figure 2. Time-resolved fibronectin binding dynamics and equilibrium fluctuations. (a) Mean adsorption behavior (black) averaged from 8 single adsorption events (violet) taken from a single rod. The deviation from a step-like form suggests a protein denaturing on the time scale of 1−2 s (inset). (b) Compared to the noise level of 0.04 nm (standard deviation) in pure water, the fluctuation amplitude increases significantly to 0.11 nm in a protein surfactant mixture (25 μg/mL fibronectin, 0.2 wt % SDS) due to equilibrium protein coverage fluctuations.

inserted into living cells,[14] providing the potential opportunity for in vivo monitoring of biomolecules.

For our experiments, rod-shaped gold nanoparticles are immobilized in a glass capillary with the possibility to introduce and change the liquid environment. The light scattering spectrum of a single gold nanorod is measured under illumination from a white light laser. The laser illuminates the particles in total internal reflection geometry such that only scattered light is picked up by the microscope and spectrally investigated (Figure 1a). With this setup, we obtain single particle scattering spectra within a few milliseconds.

Molecular adsorption processes induce only very small shifts in the plasmon resonance when compared to the plasmon line width of about 50 nm. However, we are able to determine the plasmon resonance wavelength with an accuracy of 0.03 nm by fitting the entire spectral resonance. This accuracy corresponds to 1/1000 of the spectral line width similar to the super-resolution obtained in STORM/PALM microscopy.[15,16]

To investigate molecular binding events, we introduce the blood plasma protein fibronectin (molecular weight 450 kDa). A shift in the plasmon resonance clearly indicates adsorption of fibronectin to the gold nanoparticles. The plasmon shift follows the Langmuir adsorption curves known from ensemble experiments (e.g., surface plasmon resonance sensors, SPR) with the characteristic time scaling with fibronectin concentration (Figure S1 in the Supporting Information). When we decrease the fibronectin concentration down to 1.25 μg/mL, discrete steps start to appear in the resonance wavelength time trace (Figure 1c). These discrete steps are caused by individual attaching molecules. We found that using wavelength histograms as shown in Figure 1d is the best way to systematically identify single protein binding steps. In the histogram, each Gaussian peak corresponds to a molecule attaching to the plasmon sensor. Neighboring Gaussian peaks are separated by $\Delta\lambda_{shift}$, and their integrated area yields the step time Δt_{step}. Assuming delta-like events, the width corresponds to the experimental noise level. For the experiment shown in Figure 1c, the average step height $\Delta\lambda_{shift}$ is ~0.3 nm with about Δt_{step} = 50 s between steps and a noise level of 0.07 nm. Sometimes, step identification is difficult (see also Figures S8 and S9) as expected from the small difference between step-height and noise level.

We carefully checked that the observed steps indeed correspond to single protein binding events. The attachment frequency (the inverse of the time between steps Δt_{step}) increases as expected with protein concentration and is in quantitative agreement with theoretical predictions assuming diffusion limited rates (Figure S2a). Furthermore, the distribution of adsorption events follows Poissonian statistics (Figure S2b). To validate the step height $\Delta\lambda_{shift}$, we checked if it varies with protein size. Fibronectin is a dimeric protein that can be cleaved into its monomeric constituents by tris(2-carboxyethyl)phosphine (TCEP). Indeed, the average shift or step height induced by monomeric fibronectin is about half the value as that of dimeric fibronectin (Figure S2c). As an additional validation, we follow the desorption of the proteins reported before[17] by washing with sodium dodecyl sulfate (SDS). We observe clearly pronounced desorption steps

dx.doi.org/10.1021/nl204496g | Nano Lett. 2012, 12, 1092−1095

(Figure S2d). However, the step height is significantly larger than for the adsorption steps, indicating the simultaneous desorption of clusters of proteins. The desorption process results in a plasmon resonance blue-shifted compared to the original wavelength, indicating a negative charging of the gold particles[18] by SDS. A control experiment of pure gold nanorods exposed to SDS results in a similar blue shift (Figure S3). The control experiments strongly confirm our achievement of single molecule sensitivity.

Being able to resolve single protein binding, we can try to time-resolve the adsorption process itself—information fundamentally hidden in ensemble measurements. For this, we manually superimpose and average all steps within one measurement to increase the signal-to-noise ratio further. We observe a plasmonic red-shift during the adsorption process with about 1.95 s time scale (Figure 2a). Similar observations show up on superimposed steps of other measurements (Figure S4), confirming the existence of a real physical process. We believe that this slow red-shift within one adsorption event arises from a slow denaturing of the protein on the surface, bringing it closer to the particle (Figure 2a, inset). Such denaturing of proteins near metal surfaces is, by itself, a well-known phenomenon.[19] Our method allows now for observation of the temporal evolution of this process in detail and should trigger the development of models to explain the observed denaturing time scale.

The most exciting feature of sensors with single molecule sensitivity is the window they provide to molecular dynamics, Brownian motion, equilibrium, and nonequilibrium fluctuations. Equilibrium coverage fluctuations give direct access to binding constants without mass transfer complications.[20] In addition, equilibrium fluctuations are linked to nonequilibrium properties via fluctuation−dissipation theorems.[21] The recent discovery of unexpected fluctuation theorems, e.g., the Jarzynski theorem,[22] have increased the demand for experimental techniques to study molecular fluctuations. Within our experiment, we observe equilibrium coverage fluctuations of fibronectin on the sensor surface under conditions of weak binding affinity. To adjust the binding affinity, we added both fibronectin and SDS and observed an increase in the fluctuation amplitude from 0.04 to 0.11 nm (Figure 2b). The stability of our current setup prevents us from recording time traces long enough for statistical evaluation with respect to fluctuation theorems, but the results clearly show the potential for molecular coverage analysis.

To fully understand the future potential of single plasmonic nanoparticles as molecular sensors, we investigated theoretically and experimentally the limit of the method, in particular the improvements needed for detecting smaller molecules. It is important to understand that it is not trivial to choose the optimal nanorod size since there is a trade-off of signal strength and resonance accuracy. Larger nanorods generally give stronger light scattering signals and should allow to determine the plasmon resonance with higher accuracy. (Retardation effects and radiation damping lead to increased plasmon line width at some point.) However, the sensing volume that influences the resonance position also increases with particle size (Figure 3a and Figure S5a) which decreases the perturbation caused by a single molecule. Indeed, experiments using large, medium, and small gold nanorods (50, 35, and 14 nm width) show larger median plasmon shifts for smaller particles (Figure 3b).

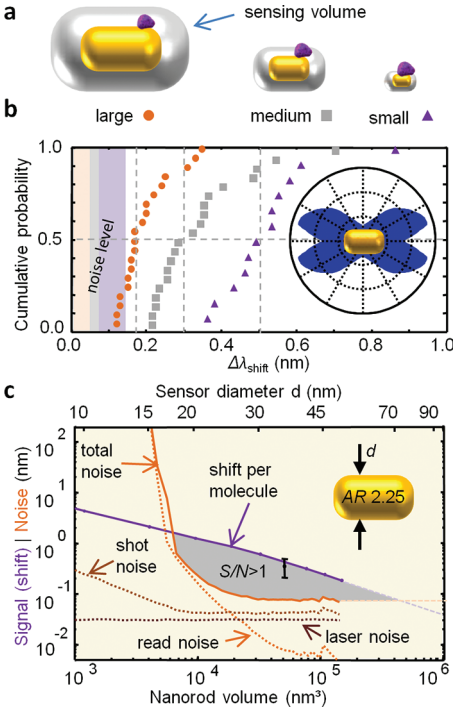

Figure 3. Optimal nanorod sensor dimensions. (a) The modification of sensing volume with particle size implies a change in occupied volume fraction. (b) Cumulative probability of measured resonance shifts per adsorbed molecule within one trace for large rods (orange, mean shift 0.17 nm), medium rods (gray, 0.30 nm), and small rods (purple, 0.51 nm). The respective noise level is shaded on the left-hand side. The large-shift tail in the cumulative distribution is caused by the position-dependent sensitivity along the rod (the inset shows a simulation for a 12 nm diameter protein on a 35 nm wide nanorod.). (c) Simulated shift induced by a 12 nm diameter adsorbing protein (purple) compared to the noise level of our setup. In the gray area, the signal-to-noise level is above one. The data point for 35 nm rods is the average shift per molecule as measured experimentally.

Using experimentally determined noise levels from our laser and camera and the sensor response (shift per molecule) calculated with the boundary element method,[23,24] we studied the signal-to-noise ratio for rods between 10 and 50 nm in width (aspect ratio (AR) 2.25). The results show an optimal size region with signal-to-noise S/N > 1 for particles with widths between 20 and 45 nm (Figure 3c). The calculated shift per molecule matches very well the measured value, confirming once more single molecule detection. The theoretical description allows us to determine the limit of plasmonic nanoparticle sensors to detect small molecules. Increasing the laser power up to a point where the absorbed light increases the particle temperature by 1 K, we could detect molecules of 4 nm diameter within the current geometry and setup using nanorods with 20 nm width. Smaller nanorods improve the detection limit even more but require much stronger lasers. Further improvements would be provided by the use of plasmonic structures with even higher sensitivity such as metamaterials,[25−27] rattles,[28] silver particles,[29] or plasmonic hot spots.[30]

Single molecule detection with individual plasmonic nanoparticles is not simply a dramatic downscaling of current sensors but a qualitative new step as it resolves molecular dynamics. With our new scheme, we can monitor desorption and adsorption processes in real time on a single molecule basis including conformational protein dynamics. Additionally, we

dx.doi.org/10.1021/nl204496g | Nano Lett. 2012, 12, 1092−1095

demonstrate its suitability for observing equilibrium coverage fluctuations. These fluctuations hold information about binding kinetics and nonequilibrium thermodynamics. Single plasmon biosensors are therefore a new tool to study fundamental phenomena on the molecular level with impact for understanding of biological processes and thermodynamics of small systems.

The dramatic improvements in signal-to-noise ratio for plasmon sensors we obtained here for our goal of single molecule detection will also improve other plasmonic sensors, e.g., 3D plasmon rulers[31] or hydrogen sensors.[32]

■ ASSOCIATED CONTENT

Supporting Information

Detailed information on materials and methods as well as results of further experiments and controls; background on simulations of the expected shift induced by protein adsorption and the setup noise; additional time traces and data on the TEM study of fibronectin. This material is available free of charge via the Internet at http://pubs.acs.org.

■ AUTHOR INFORMATION

Corresponding Author

*E-mail: Soennichsen@uni-mainz.de.

Notes

The authors declare no competing financial interest.

■ ACKNOWLEDGMENTS

A. Trügler and U. Hohenester provided support with BEM simulations. We thank H. Giessen for insightful discussions and S. Hein for help with 3D visualization. This work was financially supported by the ERC grant 259640 ("SingleSens"). I.A. was financially supported by the Carl-Zeiss Foundation and J.P. by the graduate school of excellence Materials Science in Mainz.

■ REFERENCES

(1) Henzler-Wildman, K.; Kern, D. *Nature* **2007**, *450*, 964−972.
(2) Weiss, S. *Science* **1999**, *283*, 1676−1683.
(3) Yanik, A. A.; Cetin, A. E.; Huang, M.; Artar, A.; Mousavi, S. H.; Khanikaev, A.; Connor, J. H.; Shvets, G.; Altug, H. *Proc. Natl. Acad. Sci. U. S. A.* **2011**, *108*, 11784−11789.
(4) Armani, A. M.; Kulkarni, R. P.; Fraser, S. E.; Flagan, R. C.; Vahala, K. J. *Science* **2007**, *317*, 783−787.
(5) He, L.; Oezdemir, S. K.; Zhu, J.; Kim, W.; Yang, L. *Nature Nanotechnol.* **2011**, *6*, 428−432.
(6) Nie, S. M.; Emery, S. R. *Science* **1997**, *275*, 1102−1106.
(7) Sorgenfrei, S.; Chiu, C. Y.; Gonzalez, R. L.; Yu, Y. J.; Kim, P.; Nuckolls, C.; Shepard, K. L. *Nature Nanotechnol.* **2011**, *6*, 125−131.
(8) Cui, Y.; Wei, Q. Q.; Park, H. K.; Lieber, C. M. *Science* **2001**, *293*, 1289−1292.
(9) McFarland, A. D.; Van Duyne, R. P. *Nano Lett.* **2003**, *3*, 1057−1062.
(10) Anker, J. N.; Hall, W. P.; Lyandres, O.; Shah, N. C.; Zhao, J.; Van Duyne, R. P. *Nature Mater.* **2008**, *7*, 442−453.
(11) Larsson, E. M.; Langhammer, C.; Zoric, I.; Kasemo, B. *Science* **2009**, *326*, 1091−1094.
(12) Sönnichsen, C.; Franzl, T.; Wilk, T.; von Plessen, G.; Feldmann, J.; Wilson, O.; Mulvaney, P. *Phys. Rev. Lett.* **2002**, *88*, 077402.
(13) Vahala, K. J. *Nature* **2003**, *424*, 839−846.
(14) Jain, P. K.; Huang, X.; El-Sayed, I. H.; El-Sayed, M. A. *Acc. Chem. Res.* **2008**, *41*, 1578−1586.
(15) Betzig, E.; Patterson, G. H.; Sougrat, R.; Lindwasser, O. W.; Olenych, S.; Bonifacino, J. S.; Davidson, M. W.; Lippincott-Schwartz, J.; Hess, H. F. *Science* **2006**, *313*, 1642−1645.
(16) Rust, M. J.; Bates, M.; Zhuang, X. *Nature Methods* **2006**, *3*, 793−795.
(17) Mayer, K. M.; Hao, F.; Lee, S.; Nordlander, P.; Hafner, J. H. *Nanotechnology* **2010**, *21*, 255503.
(18) Mulvaney, P.; Perez-Juste, J.; Giersig, M.; Liz-Marzan, L. M.; Pecharroman, C. *Plasmonics* **2006**, *1*, 61−66.
(19) Anand, G.; Sharma, S.; Dutta, A. K.; Kumar, S. K.; Belfort, G. *Langmuir* **2010**, *26*, 10803−10811.
(20) Lüthgens, E.; Janshoff, A. *ChemPhysChem* **2005**, *6*, 444−448.
(21) Kubo, R. *Rep. Prog. Phys.* **1966**, *29*, 255.
(22) Jarzynski, C. *Phys. Rev. Lett.* **1997**, *78*, 2690−2693.
(23) Garcia de Abajo, F. J.; Howie, A. *Phys. Rev. B* **2002**, 65.
(24) Hohenester, U.; Trügler, A. *Comput. Phys. Commun.* **2011**, *183*, 370−381.
(25) Liu, N.; Liu, H.; Zhu, S.; Giessen, H. *Nature Photonics* **2009**, *3*, 157−162.
(26) Kabashin, A. V.; Evans, P.; Pastkovsky, S.; Hendren, W.; Wurtz, G. A.; Atkinson, R.; Pollard, R.; Podolskiy, V. A.; Zayats, A. V. *Nature Mater.* **2009**, *8*, 867−871.
(27) Liu, N.; Guo, H.; Fu, L.; Kaiser, S.; Schweizer, H.; Giessen, H. *Nature Mater.* **2008**, *7*, 31−37.
(28) Khalavka, Y.; Becker, J.; Sönnichsen, C. *J. Am. Chem. Soc.* **2009**, *131*, 1871−1875.
(29) Jakab, A.; Rosman, C.; Khalavka, Y.; Becker, J.; Trügler, A.; Hohenester, U.; Sönnichsen, C. *ACS Nano* **2011**, *5*, 6880−6885.
(30) Acimovic, S. S.; Kreuzer, M. P.; Gonzalez, M. U.; Quidant, R. *ACS Nano* **2009**, *3*, 1231−1237.
(31) Liu, N.; Hentschel, M.; Weiss, T.; Alivisatos, A. P.; Giessen, H. *Science* **2011**, *332*, 1407−1410.
(32) Liu, N.; Tang, M. L.; Hentschel, M.; Giessen, H.; Alivisatos, A. P. *Nature Mater.* **2011**, *10*, 631−636.
(33) Vollmer, F.; Arnold, S. *Nat. Methods* **2008**, *5*, 591−596.
(34) Pang, Y.; Gordon, R. *Nano Lett.* **2012**, *12*, 402−406.